Science of the Total Environment 473–474 (2014) 549–564

Contents lists available at ScienceDirect

Science of the Total Environment

journal homepage: www.elsevier.com/locate/scitotenv

The dark side of the tradition: The polluting effect of Epiphany folk fires in the eastern Po Valley (Italy)

Mauro Masiol [a,b], Gianni Formenton [c], Giorgia Giraldo [d], Alberto Pasqualetto [c], Paulo Tieppo [c], Bruno Pavoni [a,*]

[a] Dipartimento di Scienze Ambientali, Informatica e Statistica, Università Ca' Foscari Venezia, Dorsoduro 2137, 30123 Venice, Italy
[b] Division of Environmental Health & Risk Management, School of Geography, Earth & Environmental Sciences, University of Birmingham, Edgbaston, Birmingham B15 2TT, United Kingdom
[c] Dipartimento Provinciale di Padova, Agenzia Regionale per la Prevenzione e Protezione Ambientale del Veneto (ARPAV), Via Ospedale 22, 35121 Padova, Italy
[d] Dipartimento Provinciale di Venezia, Agenzia Regionale per la Prevenzione e Protezione Ambientale del Veneto (ARPAV), Via Lissa 6, 30174 Mestre, Italy

HIGHLIGHTS

- The effects of thousand folk fires on the air quality were monitored.
- The levels of TC, major inorganic ions, PAH, levoglucosan and K^+ were measured.
- The daily concentrations of $PM_{2.5}$ and PM_{10} exceeded 250 and 300 μg m^{-3}.
- The dispersion of the PM was traced in Veneto (Italy) and neighboring regions.
- This study provides experimental data on the biomass burning practice.

GRAPHICAL ABSTRACT

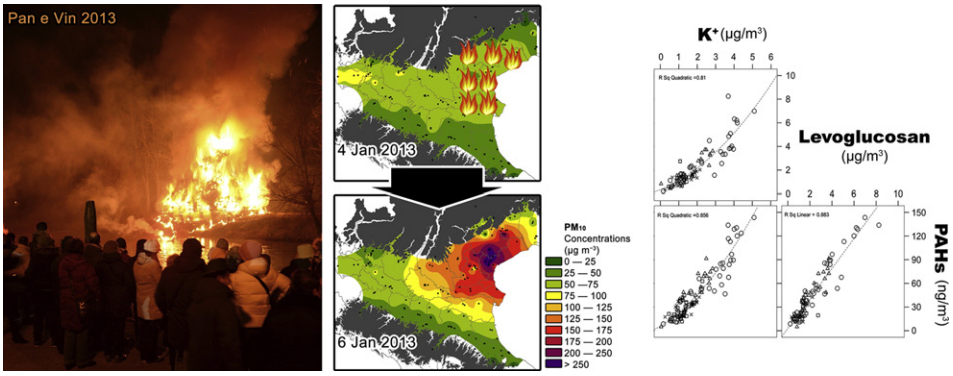

ARTICLE INFO

Article history:
Received 24 June 2013
Received in revised form 16 December 2013
Accepted 16 December 2013
Available online 4 January 2014

Keywords:
Particulate matter
Biomass burning
Levoglucosan
Polycyclic aromatic hydrocarbons
Po Valley

ABSTRACT

In the Veneto Region (Po Valley, Northeastern Italy) on the eve of Epiphany, an important religious celebration, during the night between January 5th and 6th thousands of folk fires traditionally burn wooden material. The object of this study is to characterize the 2013 episode, by monitoring the effects on the air quality in the region's lowlands. The daily concentrations of $PM_{2.5}$ and PM_{10} exceeded 250 and 300 μg m^{-3}, respectively and the PM_{10} hourly values were above 600 μg m^{-3} in many sites. The levels of total carbon, major inorganic ions, polycyclic aromatic hydrocarbons and biomass burning tracers (levoglucosan and K^+) were measured in 84 samples of PM_{10} and 38 of $PM_{2.5}$ collected at 32 sites between January 4th and 7th. Total carbon ranged from 11 μg m^{-3} before the pollution episode to 131 μg m^{-3} a day afterwards, K^+ from 0.6 to 5.1 μg m^{-3}, benzo(*a*)pyrene from 2 to 23 ng m^{-3}, and levoglucosan from 0.5 to 8.3 μg m^{-3}. The dispersion of the particulate matter was traced by analyzing the levels of PM_{10} and $PM_{2.5}$ in 133 and 51 sites, respectively, in the Veneto and neighboring regions. In addition to biomass burning the formation of secondary inorganic aerosol was revealed to be a key factor on a multivariate statistical data processing. By providing direct information on the effects of an intense and widespread biomass burning episode in the Po Valley, this study also enables some general considerations on biomass burning practices.

1. Introduction

Biomass burning (BB) from natural and human-induced fires for deforestation, agricultural waste disposal and wood-fuel use for domestic heating, is largely recognized as a significant global source of gaseous

* Corresponding author.
E-mail address: brown@unive.it (B. Pavoni).

0048-9697/$ – see front matter © 2013 Elsevier B.V. All rights reserved.
http://dx.doi.org/10.1016/j.scitotenv.2013.12.077

and particulate matter (PM) emissions (e.g., Crutzen and Andreae, 1990; Andreae and Merlet, 2001; Mayol-Bracero et al., 2001; Simoneit, 2002; Radzi et al., 2004; Akagi et al., 2011; Zhang et al., 2013). Its impact on the atmospheric chemistry, regional air quality, human health, visibility and climate is currently being amply discussed (Reid et al., 2005; Gustafsson et al., 2009; Laumbach and Kipen, 2012; Keywood et al., 2011). In particular, both wildfires during intense episodes (Saarikoski et al., 2007; Pio et al., 2008; Alves et al., 2010; Portin et al., 2012) and domestic wood burning in winter (Szidat et al., 2007; Gelencsér et al., 2007; Caseiro et al., 2009; Piazzalunga et al., 2011; Reche et al., 2012) have been identified as major sources of PM at many European locations that deserve more attention from the scientific community.

Nevertheless, in the Po Valley, which is recognized as having very high levels of many air pollutants frequently breaching the European standards for air quality (EEA, 2013), data on BB are still incomplete, many questions are still unanswered and the debate on the use of wood for domestic heating is still in progress in northern Italy. Recent studies reported that wood combustion strongly contributes to the air pollution (van Drooge and Perez Ballesta, 2009; Piazzalunga et al., 2010, 2011; Belis et al., 2011; Perrone et al., 2012; Piazzalunga et al., 2013) and the use of wood (i.e. logs, briquettes, chips and pellets) is becoming a widely used renewable alternative to methane (Pignatelli et al., 2008; European Pellet Council, 2011; Pastorello et al., 2011). Studies on the effects of intense BB pollution episodes in the Po Valley are still lacking.

This study aims to experimentally characterize an intense air pollution episode caused by the simultaneous burning of more than a thousand folk fires in the eastern Po Valley, Veneto Region, in January 2013. The main goals are to quantify particulate pollution and characterize variations in the levels of some well-known BB tracers, such as levoglucosan, K^+ and certain polycyclic aromatic hydrocarbons (PAHs) during the period sampled. The concentration ratios between pairs of PM-bound compounds including BB tracers are used to investigate the PM composition before, during and after the event. Finally, the dispersion of the PM pollution in the surrounding regions is examined to assess the extent of the episode.

2. Study area and Epiphany fires

The concurrent presence of numerous emission sources and particular weather conditions that favor pollutant accumulation is responsible for the worrying air quality in the Po Valley, especially in winter. The anthropogenic pressure includes large cities separated by a continuum of scattered urban settlements, roads with heavy traffic, industrial areas, and farmland. The particular weather conditions are determined mainly by the orographic arrangement of Alps and Apennines that protect the valley from long distance winds and favor extended periods of low temperatures, winds and mixing layers and frequent temperature inversions (e.g., Tomasi, 1983; Vecchi et al., 2004, 2007; Pecorari et al., 2013).

The Veneto Region lies in the eastern Po Valley and extends over ~$18.4 \cdot 10^3$ km^2 hosting a population of ~4.9 million. Its territory includes the northern alpine environments (29% of the total surface area), the intermediate hill areas (15%), the heavily anthropized plains to the south (56%) and the eastern ~95 km long coastlines (Fig. 1). In 2011, the standards fixed by the European directives were exceeded at many sites monitored by the Environmental Protection Agency of Veneto (ARPAV): i.e. the annual limits for PM_{10} (40 μg m^{-3}) at 50% of the sites, the target values of $PM_{2.5}$ (25 μg m^{-3}) at 78%, the PM_{10}-bound benzo(*a*)pyrene (1 ng m^{-3}) at 53%, the annual limit for NO_2 (40 μg m^{-3}) at 20% of the sites. At all the stations the long-term objective for ozone for the protection of human health (ARPAV, 2012) was critically breached. According to data published by the European Environment Agency in the Veneto, at least 10–15 premature deaths per year per 10,000 population are attributable to $PM_{2.5}$ pollution (de Leeuw and Horálek, 2009). It is therefore urgently necessary to find quick and effective solutions to reduce the population's exposure to harmful air pollutants.

Following the popular Venetian tradition, large piles of wood and branches are burned on the eve of Epiphany, the night of January 5th–6th . This event, called "*Panevin*", "*vècia*" or "*pìroła-pàroła*" and probably deriving from pre-Christian rites, marks the beginning of the new year and it is celebrated regularly all over the region. In the past small piles of wood were prepared in front of the farmhouses, recently many local authorities, parishes and various local associations have been organizing the event. The real number of fires in Veneto is unknown, but it is reasonable to assume that about thousand piles are burnt every year. The tradition is particularly strong in the provinces of Treviso and Venice (Fig. 1).

Piles can be large in size (up to 10 m high and 4 m wide) and are made of various wooden materials, from dry branches to green underbrush weeds, from hardwood to chipboard and old wooden objects, many of which may be painted, varnished or contain metal or plastic components. In most of the Veneto, the 2013 fires started on January 5th at 18:00 local time and ended at about midnight, when the flames died out. Because these fires are poorly controlled, the organic material easily pyrolyzes and large amounts of soot are produced.

3. Materials and methods

3.1. Sampling

A set of 122 daily samples (38 $PM_{2.5}$ and 84 PM_{10}) was collected simultaneously from January 4th to 7th 2013 at 32 sites in the Veneto categorized as rural (RUR, 3 sites), suburban (SUB, 6), urban backgrounds (URB, 14), industrial (IND, 5) and traffic hot-spots (TRA, 4). The sampling campaign covered 6 provinces: Belluno (BL), Treviso (TV), Vicenza (VI), Venice (VE), Padova (PD) and Rovigo (RO). At least one site was selected as an urban background in the capital of each province, namely sites 4, 9, 12, 17, 22 and 30 located in Belluno, Treviso, Vicenza, Venice-Mestre, Padova and Rovigo, respectively. The sites were identified by a number, the initials for the province and their category. The map of selected sites is shown in Fig. 1, while Table 1 summarizes some of sites' characteristics. Sites are included in the monitoring network of the Veneto Agency for the Environmental Control (ARPAV) and were carefully placed in areas representative of each category. For example, urban background sites are broadly representative of city-wide levels of air pollutants, rural background stations are not directly influenced by roads with traffic and/or urban and industrial settlements. Since the event being studied is by nature occasional, unpredictable, and outside the authorities' control, it is impossible to know the number of fires and whether or not they were lit in the vicinity of the sampling sites. Furthermore, it is not obvious that inside the cities more fires were burnt than in suburban or rural areas. The purpose of this study is to describe the episode on a large regional scale and therefore the sampling sites should be considered representing a portion of territory rather than a specific category.

3.2. Experimental

Samplings (24-h starting at 0:00 local time) were carried out according to the EN 14907:2005 (CEN, 2005a) and EN 12341:1998 (CEN, 1998) standards for $PM_{2.5}$ and PM_{10}, respectively, using 47 mm Ø quartz fiber filters (Whatman QMA, GE Healthcare). PM_x masses were measured gravimetrically after conditioning at 20 ± 1 °C and 50 ± 5% relative humidity for 48 h. Some samples were also tested automatically using samplers based on the beta gauge method. Validation experiments were conducted on the gravimetric and automatic procedures before the sampling campaign. In addition, several tests were also performed routinely (at least 1 test every week) to keep a constant check on the automatic samplers. Pairs of filters were measured with both methods and the results were checked to ensure they were

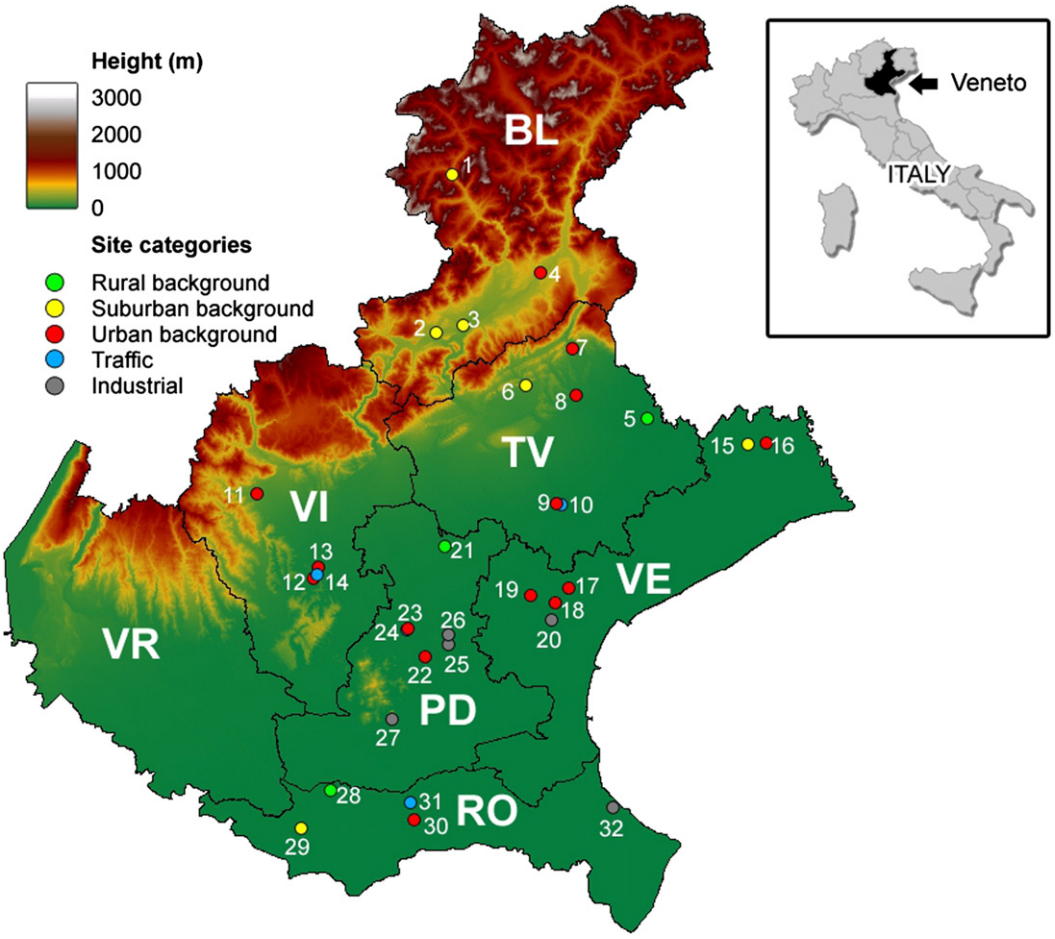

Fig. 1. Study area. Provinces of Veneto: BL = Belluno; TV = Treviso; VI = Vicenza; VE = Venice; PD = Padova; RO = Rovigo. Major cities of the Po Valley used for the MLRA are also shown: BO = Bologna; MO = Modena; MI = Milan.

within the variation margins imposed by the technical protocols adopted in UNI EN 12341:2001. There was a generally good agreement between the two methods. Each sampled filter was punched in 3 circular subsamples (diameter: 16 mm), that were stored in the dark at −20 °C to prevent any photochemical reactions, evaporative losses or biological processes.

The first subsample was analyzed to quantify the total carbon (TC) content using a Shimadzu (Japan) TOC-V CPH coupled with a SSM-5000A module. TC was quantified by a catalyzed oxidative conversion to CO_2 at 900 °C, then analyzed with a NDIR detector. Anhydrous D(+)glucose (Carlo Erba, ACS) was used as a standard to test the linearity and calibrate the instrumental responses. The quality and accuracy of the quantitative analyses were checked by analyzing the NIST SRM 1649a. A 6.4% relative uncertainty was estimated for this method in accordance with the UNI ISO 3534-1 norm.

The second subsample was ultrasonically extracted with 20 mL MilliQ water (Millipore, USA) in capped vials maintained in the ultrasonic bath for 20 min at a temperature <30 °C to avoid evaporation or nitrate artifact formation. Resulting solutions were then filtered using 0.45 μm PTFE membranes and injected into two ion chromatographic systems using conductivity detection (Metrohm, Switzerland) to quantify the concentrations of five anions (F^-, Cl^-, NO_3^-, PO_4^{3-}, SO_4^{2-}) and five cations (Na^+, NH_4^+, K^+, Mg^{2+}, Ca^{2+}). Anions were separated on a Metrosep A Supp 7-250/4.0 column applying a isocratic eluent flow (0.8 mL min^{-1}) of 360 mM Na_2CO_3 (Sigma-Aldrich, ACS ≥ 99.8%). Cations were measured using a Metrosep C 3-150/4.0 column and a 1 mL min^{-1} isocratic flow of 3 mM ultrapure HNO_3 (Fluka, TraceSELECT, ≥69%). Single-ionic standards were used to test the linearity and calibrate the instrumental responses. A routine analytical check was made by using certified liquid standards (Fluka, TraceCERT) diluted in MilliQ water. The relative standard deviation of repeated analyses was <5% for each ion.

The third subsample was ultrasonically extracted for 15 min in 5 mL of acetonitrile (Sigma-Aldrich, HPLC grade ≥99.9%) and filtered with 0.2 μm porosity PTFE membranes. An aliquot (5 μL) was injected into a 2695 series Alliance HPLC (Waters, USA) interfaced with a 2475 multi λ fluorescence detector for the determination of eight polycyclic aromatic hydrocarbons (PAHs) selected from the EPA list for being mostly in the PM phase: benz(*a*)anthracene (BaA), chrysene (Chry), benzo(*b*)fluoranthene (BbF), benzo(*k*)fluoranthene (BkF), benzo(*a*)pyrene (BaP), indeno(1,2,3-*c*,*d*)pyrene (IP), dibenzo(*a*,*h*)anthracene (DBahA) and benzo(*g*,*h*,*i*)perylene (BghiP). HPLC set-up was: RP chromatographic column (Supelco, LC-PAH 15 cm × 3 mm, 5 μm) at a temperature of 25 °C, mobile phase consisting in a variable mixture of ultrapure H_2O and acetonitrile at a flow rate of 0.5 mL min^{-1}. A reference material (PAH mixture, Ultra Scientific) was used to test the linearity and calibrate the instrumental responses. The analytical quality was routinely checked by analyzing the NIST SRM 1648b. The relative uncertainty, at 95% confidence level, calculated according to EN 15549:2008 (CEN, 2008), was ±11% for B(a)P; similar uncertainties were calculated for other PAHs determined with the same technique in accordance with the ISO 16362:2005 (ISO, 2005). Some additional information about the adopted analytical methods is provided as SI, Table 1.

The remaining aliquot of the filter was treated with the Supelco derivatizing solution BSA + TMCS + TMSI 3:2:3 (Sylon BTZ) for 30 min at 70 °C. After 2 min, 1 mL MilliQ water and 1 mL hexane (Fluka, for residue analysis ≥99%) were added to complete the extraction and to eliminate the excess of silanizing agent. The hexane fraction

Table 1
Characteristics of the selected sapling sites. ID refers to the site number used in the text. Categorization: RUR = rural background; SUB = suburban background; URB = urban background; IND = industrial; TRA = traffic hot-spot. Latitude (Nord) and longitude (East) are in WGS84.

ID	Province	Site name	Category	Longitude	Latitude	Daily PM samples	Other automatic measurements
1	BL	Cencenighe Agordino	SUB	11.968	46.350	PM_{10}	–
2	BL	Area feltrina	SUB	11.905	46.030	$PM_{2.5}$, PM_{10}	NO, NO_2, NO_x, O_3
3	BL	Cesiomaggiore-Busche	SUB	11.986	46.042	PM_{10}	Benzene, O_3
4	BL	Belluno-Centro	URB	12.218	46.143	$PM_{2.5}$, PM_{10}	CO, NO, NO_2, NO_x, O_3,SO_2
5	TV	Mansué	RUR	12.510	45.837	$PM_{2.5}$	NO, NO_2, NO_x, O_3
6	TV	Pieve di Soligo	SUB	12.162	45.916	PM_{10}	–
7	TV	Vittorio Veneto	URB	12.302	45.986	PM_{10}	CO, NO, NO_2, NO_x, O_3,SO_2
8	TV	Conegliano	URB	12.307	45.890	$PM_{2.5}$	NO, NO_2, NO_x, O_3
9	TV	Treviso-Via Lanceri Novara	URB	12.238	45.672	PM_{10}	NO, NO_2, NO_x, O_3,SO_2
10	TV	Treviso-Porta San Tommaso	TRA	12.251	45.670	PM_{10}	–
11	VI	Schio	URB	11.368	45.714	PM_{10}	CO, NO, NO_2, NO_x, O_3,SO_2
12	VI	Vicenza-Quartiere Italia	URB	11.539	45.560	$PM_{2.5}$	NO, NO_2, NO_x, O_3
13	VI	Vicenza-Ferrovieri	URB	11.524	45.539	PM_{10}	CO, NO, NO_2, NO_x, O_3
14	VI	Vicenza-San Felice	TRA	11.533	45.545	PM_{10}	CO, NO, NO_2, NO_x,SO_2
15	VE	Portogruaro-Summaga	SUB	12.799	45.777	PM_{10}	–
16	VE	Portogruaro-Via Manzoni	URB	12.854	45.775	PM_{10}	–
17	VE	Mestre-Parco Bissuola	URB	12.261	45.498	$PM_{2.5}$, PM_{10}	Benz, NO, NO_2, NO_x, O_3,SO_2
18	VE	Mestre-Via Beccaria	URB	12.221	45.470	PM_{10}	NO, NO_2, NO_x
19	VE	Spinea	URB	12.150	45.488	PM_{10}	Benzene, CO, NO, NO_2, NO_x, O_3,SO_2
20	VE	Malcontenta	IND	12.209	45.435	$PM_{2.5}$, PM_{10}	CO, NO, NO_2, NO_x, SO_2
21	PD	Santa Giustina in Colle	RUR	11.909	45.594	PM_{10}	CO, NO, NO_2, NO_x, O_3
22	PD	Padova-Mandria	URB	11.841	45.371	$PM_{2.5}$	CO, NO, NO_2, NO_x, O_3,SO_2
23	PD	Rubano-Via Strasburgo	URB	11.794	45.429	$PM_{2.5}$	CO, NO, NO_2, NO_x, O_3,SO_2
24	PD	Rubano-Via Rossi	TRA	11.788	45.426	PM_{10}	CO, NO, NO_2, NO_x, O_3,SO_2
25	PD	Padova-Industrial 1	IND	11.909	45.395	$PM_{2.5}$, PM_{10}	CO, NO, NO_2, NO_x, O_3,SO_2
26	PD	Padova-Industrial 2	IND	11.907	45.415	$PM_{2.5}$, PM_{10}	CO, NO, NO_2, NO_x, O_3,SO_2
27	PD	Monselice	IND	11.737	45.246	PM_{10}	–
28	RO	Badia Polesine	RUR	11.554	45.103	PM_{10}	CO, NO, NO_2, NO_x, O_3,SO_2
29	RO	Trecenta	SUB	11.467	45.030	PM_{10}	CO, NO, NO_2, NO_x, O_3,SO_2
30	RO	Rovigo-Borsea	URB	11.790	45.039	PM_{10}	NO, NO_2, NO_x, O_3
31	RO	Rovigo-Largo Martiri	TRA	11.782	45.074	$PM_{2.5}$	Benzene, CO, NO, NO_2, NO_x, O_3,SO_2
32	RO	Porto Viro-Porto Levante	IND	12.364	45.049	PM_{10}	Benzene, CO, NO, NO_2, NO_x, O_3,SO_2

was then analyzed on a GC–MS Trace DSQ (Thermo, USA) using a Restek Rxi-5Sil MS capillary column (30 m × 0.25 mm inner diameter, 0.25-μm film thickness) to quantify the methyl derivative of the monosaccharide levoglucosan (1,6-anhydro-β,D-glucopyranose), which is a well-known marker of hemicellulose pyrolysis (Shafizadeh, 1968; Simoneit, 2002) and is widely used as a BB tracer (e.g., Fine et al., 2001; Puxbaum et al., 2007; Mazzoleni et al., 2007; Caseiro et al., 2009). Pure levoglucosan (Sigma-Aldrich, 99%) was used to calibrate the instrumental responses; sedoheptulose anhydride monohydrate (Sigma-Aldrich, >99%) was used as an internal standard. The repeatability relative standard deviation of levoglucosan determination was <12%.

3.3. Automatic measurements

At a number of selected sites, other chemical parameters were automatically determined on an hourly or bihourly basis using standard methods: EN 14626:2012 for CO (CEN, 2012a); EN 14211:2012 for NO, NO_2, NO_x (CEN, 2012b); EN 14212:2012 for SO_2 (CEN, 2012c); EN 14625:2012 for O_3 (CEN, 2012d); EN 14662-3:2005 for benzene (CEN, 2005b); PM_{10} and $PM_{2.5}$ were quantified with automatic beta gauge samplers. A comprehensive list of the parameters measured at each site is provided in Table 1.

3.4. Meteorological data

Weather data on a regional scale including wind vectors, surface pressures, Pasquill stability classes, air temperatures at ground and planetary boundary layer heights were obtained from the GDAS1 archive at the Air Resources Laboratory (NOAA, USA). Details of the model adopted are reported elsewhere (NCEP, 2013). Maps of meteorological parameters were computed using the web-based 'archived model graphics' on the NOAA/READY website (http://www.ready.noaa.gov, Rolph, 2013). Forward air mass trajectories were simulated during the hours affected by the BB episode using the NOAA/ARL HYSPLIT version 4 model (Draxler and Rolph, 2013) and the NCEP/NCAR Reanalysis data. The HYSPLIT setup was: 48 h forward trajectory, starting height at 200 m agl, i.e. within the mixing layer. On a local-scale, micro-meteorological data (air temperature, solar radiation, relative humidity, atmospheric pressure, precipitation and the average speeds of prevailing winds) were recorded by ARPAV as close as possible to the sampling sites using automatic instruments.

4. Results and discussion

4.1. Weather conditions

Meteorological conditions had a key role in the accumulation/removal/dispersion of air pollutants during the study period. GDAS1 data generally showed high pressures (average 1022 hPa in the plain area), low prevailing wind regimes at ground blowing from N–NW, typical wintertime air temperatures ranging from ~1 °C at night-time to ~7 °C in daylight hours and no precipitation events. The height of the planetary boundary layer, a key parameter defining the volume of air in the lower troposphere potentially involved in the dilution of pollutants emitted at ground, never exceeded 250–300 m with the lowest levels during the night in the southwestern part of the region. The Pasquill classes, which provide an estimation of the atmospheric stability, were steadily neutral. Meteograms and maps of winds, surface temperatures, and mixing layer heights are provided as SI, Figs. 1–4. On a local-scale, weather conditions were confirmed by experimental data collected near the sampling sites: air temperatures in the plain were within the normal ranges recorded in January with daily averages from 2 to 7 °C and atmospheric circulation generally characterized by slow winds (daily averages of ~1 m s^{-1}) (SI Figs. 5–6).

All the weather conditions suggested a limited dispersion power of the atmosphere during the study period and therefore the possible

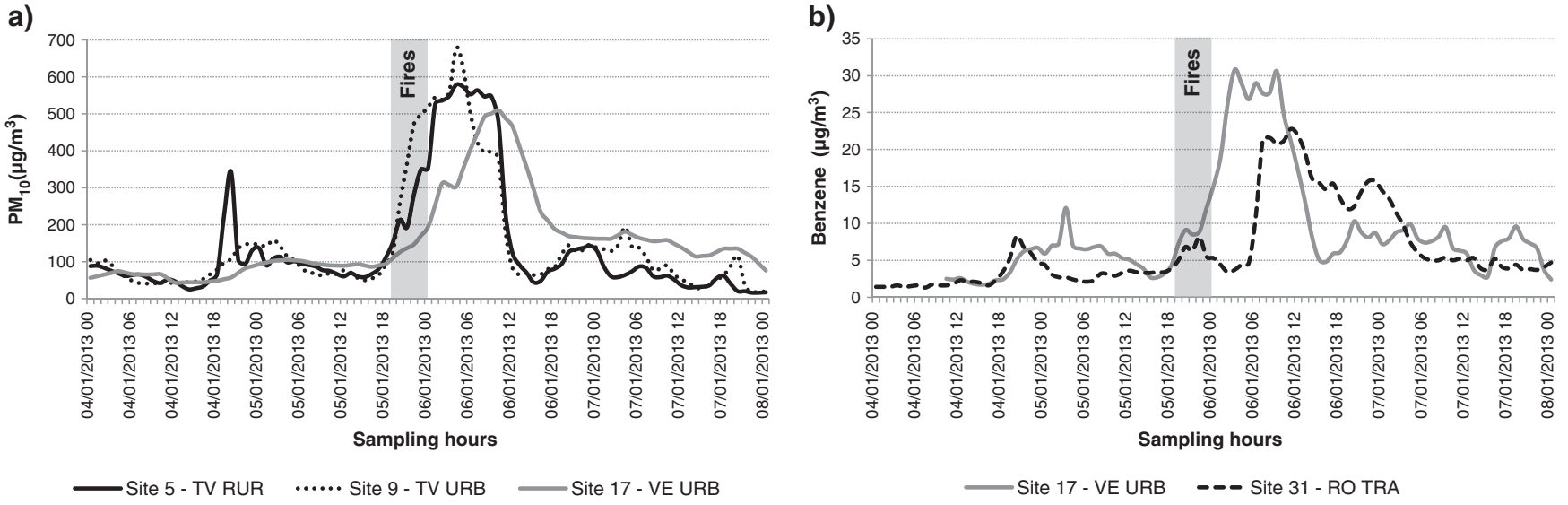

Fig. 2. a) Hourly concentrations of PM_{10} recorded in RUR and URB sites in the provinces of TV and VE and (b) hourly concentrations of benzene in Venice-Mestre (site 17, URB) and Rovigo (site 31, TRA). The hours of folk fire burning are also highlighted.

Table 2
Statistics (mean, minimum, maximum) of $PM_{2.5}$, PM_{10} and their analyzed components for the whole region. Data are grouped by province.

Date			PM(x)	F^-	Cl^-	NO_3^-	PO_4^{3-}	SO_4^{2-}	Na^+	NH_4^+	K^+	Mg^{2+}	Ca^{2+}	Σions	TC	Levoglucosan	BaA	Chry	BbF	BkF	BaP	DBahA	BghiP	IP	Σ_8PAHs
			μg m^{-3}														*ng* m^{-3}									
04/01/2013	$PM_{2.5}$	Mean	56	0.1	0.5	9.8	0.3	1.9	0.5	3.0	1.2	0.1	0.3	18	20	1.6	2.6	4.2	4.6	2.1	5.0	0.3	3.7	3.8	26
		Minimum	33	0.1	0.1	2.9	0.2	0.6	0.4	0.7	0.7	0.1	0.3	7	14	0.8	1.6	2.7	2.7	1.2	2.6	0.2	2.1	1.2	15
		Maximum	71	0.2	0.8	18.6	0.5	3.3	1.0	6.2	1.8	0.3	0.6	30	29	2.7	4.4	6.1	6.5	3.1	7.5	0.5	5.3	6.4	39
	PM_{10}	Mean	64	0.1	0.6	10.8	0.3	2.1	0.5	2.9	1.2	0.1	0.8	19	20	1.1	2.9	4.4	4.5	2.2	4.6	0.6	3.4	4.1	27
		Minimum	15	0.1	0.1	0.5	0.2	0.7	0.4	0.1	0.5	0.1	0.3	3	9	0.5	0.7	1.4	2.0	0.9	1.6	0.1	0.3	2.1	10
		Maximum	95	0.2	1.9	18.8	0.5	4.2	1.0	6.0	2.3	0.3	3.2	31	33	1.7	8.0	10.7	10.2	5.0	11.5	5.5	7.8	9.1	63
05/01/2013	$PM_{2.5}$	Mean	83	0.1	0.8	12.8	0.3	2.7	0.5	4.3	1.6	0.1	0.3	23	31	1.8	4.9	7.1	7.1	3.2	7.7	0.5	5.5	6.3	42
		Minimum	30	0.1	0.1	3.1	0.2	0.6	0.4	0.6	0.9	0.1	0.3	7	15	0.9	1.8	3.3	3.5	1.5	3.0	0.2	2.7	2.4	19
		Maximum	134	0.2	1.6	19.3	0.5	4.1	1.0	6.3	2.3	0.3	0.6	33	55	2.9	12.2	12.4	11.2	5.0	13.3	0.8	8.8	10.6	72
	PM_{10}	Mean	99	0.1	1.1	13.9	0.3	3.3	0.5	4.1	1.8	0.1	0.6	27	35	2.2	4.9	8.2	7.3	3.3	8.0	0.5	5.7	6.8	45
		Minimum	6	0.1	0.1	0.2	0.2	0.3	0.4	0.1	<0.1	0.1	0.3	2	4	0.8	0.6	0.7	0.9	0.5	1.0	0.2	0.8	0.4	5
		Maximum	166	0.2	2.2	19.6	0.5	7.4	1.0	6.3	2.8	0.3	2.6	53	64	3.7	11.4	20.1	13.2	6.2	16.6	0.9	10.3	12.9	91
06/01/2013	$PM_{2.5}$	Mean	149	0.1	2.2	15.3	0.3	3.7	0.5	5.5	2.6	0.1	0.3	31	60	3.0	9.1	14.0	10.9	4.7	11.2	0.7	7.8	8.6	67
		Minimum	22	0.1	0.1	1.8	0.2	0.3	0.4	0.2	0.5	0.1	0.3	4	11	1.1	1.1	2.1	2.5	1.2	2.6	0.2	2.1	1.0	13
		Maximum	263	0.2	6.1	23.3	0.5	7.3	1.0	9.8	4.0	0.3	0.6	49	113	6.3	24.3	24.2	19.7	8.1	22.1	1.2	12.9	16.2	129
	PM_{10}	Mean	177	0.1	2.6	16.4	0.3	4.9	0.6	5.7	2.9	0.2	0.6	35	70	3.5	9.8	16.9	11.7	4.9	12.0	0.7	8.0	9.7	74
		Minimum	14	0.1	0.1	0.2	0.2	0.6	0.4	0.1	0.2	0.1	0.3	5	6	0.2	0.9	1.4	1.6	0.8	1.7	0.1	1.4	0.7	9
		Maximum	313	0.3	5.7	24.0	0.5	9.4	1.0	9.5	5.1	0.3	2.3	63	131	8.3	22.5	37.4	21.5	8.9	23.3	1.3	14.2	18.1	143
07/01/2013	$PM_{2.5}$	Mean	68	0.1	0.7	10.5	0.3	2.5	0.6	3.8	1.2	0.1	0.3	20	25	1.0	2.4	4.4	4.3	1.9	4.1	0.3	3.3	3.8	24
		Minimum	26	<0.1	0.1	3.1	0.2	0.6	0.4	0.7	0.5	<0.1	0.3	6	13	0.4	1.1	2.1	2.5	1.0	1.8	0.1	2.0	2.2	14
		Maximum	115	0.2	1.7	16.7	1.0	4.5	1.6	6.3	2.1	0.3	0.6	32	46	1.7	5.0	9.2	7.4	3.0	6.8	0.4	4.9	6.0	43
	PM_{10}	Mean	80	0.1	1.3	12.4	0.3	3.0	0.7	4.3	1.2	0.1	0.5	24	26	1.2	2.5	4.5	4.2	1.9	3.9	0.4	3.2	3.8	24
		Minimum	20	0.1	0.1	0.4	0.2	0.7	0.4	0.1	0.3	0.1	0.3	5	7	0.3	0.3	0.6	1.7	0.8	1.1	0.1	0.1	1.4	11
		Maximum	144	0.2	4.9	18.2	0.5	4.8	1.9	6.8	2.1	0.3	1.9	38	48	2.2	6.0	10.0	8.2	3.5	8.0	2.4	5.8	6.7	49

accumulation of pollutants emitted by the burning fires. The prevalence of light winds from the N–NW also indicated a southward slow movement of polluted air masses. In most sites the relative humidity exceeded 90% (SI Fig. 7), creating favorable conditions for the formation of secondary ammonium nitrate (Squizzato et al., 2013).

Some additional parameters were also recorded to account for potential photo-, thermo-, and chemical oxidation in the atmosphere of organic compounds, such as PAHs (Arey and Atkinson, 2003) and levoglucosan (Hennigan et al., 2010): temperatures were relatively low, solar radiation reached hourly peaks of 330 W m^{-2}, O_3 and NO_2 levels never exceeded 60 μg m^{-3} (SI Figs. 8 and 9). On this basis, the processes leading to the destruction and oxidation of PM-bound organics were estimated to be negligible during the study period.

4.2. Short-term effects

The effects of the fires became evident shortly after the piles were lit. Fig. 2a shows the hourly concentrations of PM_{10} recorded in RUR and URB sites in the TV and VE districts. The rapid increase in the PM levels on January 5th at 19:00 was evident, with values reaching ~700 μg m^{-3}, i.e. up to 7 times above the levels recorded before the episode and ~18 times higher than the annual average concentration. The PM_{10} concentrations remained very high for almost a day (~20 h), until January 6th at 15:00, when they dropped to levels similar to those recorded before the fires were lit.

Automatic samplings have also measured significant increases in benzene in conjunction with the event (Fig. 2b): concentrations of 30 μg m^{-3} were recorded in Venice-Mestre, i.e. 7 times the levels commonly recorded in January. This benzene production from biomass combustions has been reported by numerous authors: e.g., Koppmann et al., 2005; Muhle et al., 2007; Akagi et al., 2011; Lewis et al., 2013. It is worth noting that the levels of benzene measured in Venice-Mestre were recorded in the hours immediately after the fire event (simultaneously with the PM_{10} peaks), whereas the highest values measured in Rovigo (approximately 60 km SW) were observed on January 7th at around 7:00, i.e. about 12 h after the fires. Although there is no official census of the fires, and virtually any town, village, parish, farmhouse or single house can burn their own fire, without any control by the authorities, it is well known that this tradition is very strong in the VE and TV districts. So, we can reasonably assume that the peak in Rovigo was the result of the dispersion of benzene produced in the districts of Venice and Treviso, located upwind in the north-east, where more fires were probably lit. This is consistent with the hypothesized movement of air masses southwards due to the slow winds recorded and provides a first important indication on the pollutant dispersion. Increases in other gaseous pollutants measured (CO, NO_x, SO_2, ozone) were not so evident (data provided as SI, Figs. 8–11).

4.3. Overview on $PM_{2.5}$ and PM_{10} pollution

Table 2 summarizes some statistics (mean, minimum, maximum) of the compounds analyzed for the whole region, while the daily distributions of $PM_{2.5}$ and PM_{10} recorded all over the study area are shown as boxplots in Fig. 3. On a regional-scale, $PM_{2.5}$

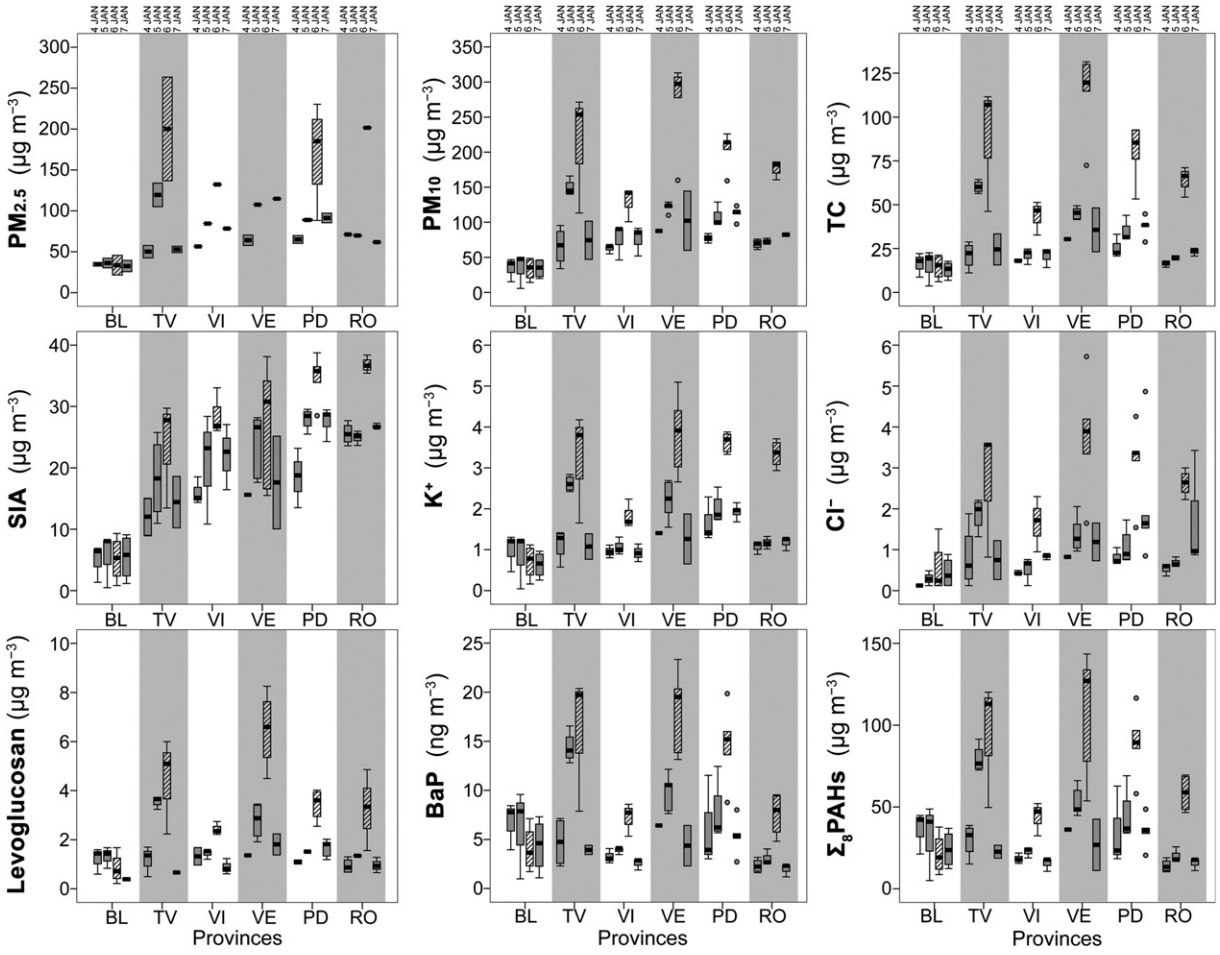

Fig. 3. Daily distributions of $PM_{2.5}$, PM_{10} and PM_{10}-bound compounds recorded in the 6 provinces investigated in this study. Boxes represent the 25–75 percentile ranges, the internal lines are the medians, whiskers are the non-outlier ranges; dots are outliers. Note that box-plots of January 6 are highlighted with a texture. SIA = secondary inorganic aerosol, i.e. sum of nitrate, sulfate and ammonium.

concentrations varied between 22 and 263 μg m^{-3} with the lowest level in the districts of BL (range 22–46 μg m^{-3}) and the highest in TV (42–263 μg m^{-3}). Similarly, PM_{10} levels ranged from 6 to 313 μg m^{-3} with the highest concentrations in the provinces of VE and TV and the lowest in BL. Results also show an evident increase in the levels of both $PM_{2.5}$ and PM_{10} on January 6th, with concentrations up to 4 times higher than those on January 4th. By applying the nonparametric Kruskal–Wallis analysis of variance by ranks, the increase in $PM_{2.5}$ and PM_{10} during the study period was generally significant ($p < 0.05$) for January 6th in all provinces except BL, where no significant differences were found. The tradition of burning Epiphany fires is less widespread in mountain communities and the effects are consequently lower. The pollution event was recorded in the lowlands (VE, TV), while no significantly abnormal concentrations were found in the alpine valleys of the province of BL, located upwind from TV and VE.

Masiol et al. (2013) recently reported that PM_{10} and PAH air pollution is quasi-uniformly in the Veneto and showed that the levels of these pollutants correlate well at most sites and in particular in the urban and suburban background sites of this study with other similar sites and demonstrated that PM_x levels have similar patterns in most of the Po Valley. Based on this evidence, a preliminary investigation was carried out to see if PM_x levels followed similar spatial variations over the whole Po Valley. This was done by correlating $PM_{2.5}$ and PM_{10} concentrations measured in the Veneto and in various other sites in the neighboring regions of the Po Valley (Lombardy, Emilia-Romagna, Friuli-Venezia Giulia). For the purpose of this study, the data considered covered the cold season (November 2012–February 2013, ~120 days), but outliers, including the period of study, were removed. The results (SI Table 4) reveal significant ($p < 0.05$) correlations between urban and suburban background sites used in this study and other similar sites and demonstrate that PM_x levels have similar patterns in most of the Po Valley. The increases in the levels of $PM_{2.5}$ and PM_{10} during the episode were then assessed by reconstructing the values of atmospheric particulate matter without the lighting of fires. The estimation was performed for the province capitals or, if not available, for other major cities through a multiple linear regression analysis (MLRA) using each time the PM_x data of a city in Veneto as dependent variable and PM_x data of some similar stations located in neighboring regions not affected by the pollution episode as independent variables. The sites used as independent variables for $PM_{2.5}$ include urban backgrounds in major cities of the Po Valley (Bologna, Modena, Milan) plus a site in the BL province, which was not affected by the episode. For PM_{10}, another site in the city of Udine was added. Results are given as SI Fig. 12 and show that the increases in $PM_{2.5}$ concentrations ($\Delta PM_{2.5}$) in the major cities of Veneto on January 6th were as follows (increase ± MLRA standard error): Conegliano (site 8, URB, 105 ± 13 μg m^{-3}); Vicenza (site 12, URB, 91 ± 12 μg m^{-3}); Venice-Mestre (site 17, URB, 235 ± 48 μg m^{-3}); Padova (site 22, URB, 148 ± 16 μg m^{-3}); Rovigo (site 31, TRA, 158 ± 13 μg m^{-3}). The increases in PM_{10} (ΔPM_{10}) were: Treviso (site 9, TV, 152 ± 20 μg m^{-3}), Vicenza (site 14, TRA, 66 ± 10 μg m^{-3}), Venice-Mestre (site 18, URB, 202 ± 17 μg m^{-3}), Padova (134 ± 27 μg m^{-3}) and Rovigo (site 30, URB, 113 ± 12 μg m^{-3}).

Although the sampling sites are not the same for PM_{10} and $PM_{2.5}$, SI Fig. 12 also suggests that the increases in particulate matter pollution were generally higher for the fine fraction than for PM_{10}. As expected, the greatest increases were recorded in the provinces of TV and VE. The ΔPM_x values estimated for January 4th were around zero at all the sites, while the highest ΔPM_x levels were always found on January 6th, followed by January 5th. On January 7th, the ΔPM_x values were low again (~0) at many sites, showing that the effect of the pollution had almost disappeared, whereas in Venice-Mestre and Padova the ΔPM_x remained significantly elevated. A more complete discussion on the dispersion of pollutants over the days following the event is provided further on.

4.4. Chemical speciation

Results of the PM_{10} chemical speciation are given as boxplots in Fig. 3, while Table 2 summarizes some statistics (mean, minimum, maximum) for the whole region. The chemical compositions of $PM_{2.5}$ show very similar patterns. In the BL province, which was not affected by the pollution episode, TC was the main PM component with concentrations varying from 11 to 21 μg m^{-3} (47–53% of the total particulate mass) and from 4 to 23 μg m^{-3} (34–66%) in $PM_{2.5}$ and PM_{10} samples, respectively. The sums of the inorganic ions analyzed in both fractions were in the range 4–12 μg m^{-3} (19–30%) and 2–12 μg m^{-3} (20–37%), respectively, and mainly consisted of nitrate, sulfate and ammonium. Levoglucosan and K^+ were in the range 0.4–1.3 μg m^{-3} and 0.5–1.1 μg m^{-3} in $PM_{2.5}$ and PM_{10}, respectively. BaP varied from 2.6 to 8.1 ng m^{-3} and the sum of all analyzed PAH congeners (Σ_8PAHs) ranged from 13 to 40 ng m^{-3}. As for the particulate matter, no significant build-up of TC, ions and BB tracers was recorded in the province of BL during the episode. In contrast, a slight decrease of the concentrations of the PM components was noted precisely on January 6th.

In all the remaining provinces affected by the event, the mass concentrations of TC, K^+, Cl^-, PAHs and levoglucosan were very high between January 5th and 6th. In particular, the highest values of TC were attained in the province of Venice (peak of 131 μg m^{-3}), K^+ (5.1 μg m^{-3}), Cl^- (6.1 μg m^{-3}), levoglucosan (8 μg m^{-3}), BaP (23 ng m^{-3}) and Σ_8PAHs (143 ng m^{-3}). As shown in Fig. 3, during the episode, in the provinces of TV and VE the most relevant increases in TC, K^+, Cl^-, levoglucosan and PAH concentrations were observed, whereas the province of RO recorded the highest levels of secondary inorganic aerosol (SIA) components, i.e. the sum of nitrate, sulfate and ammonium.

The effects of the episode on the major PM components were identified by applying the Kruskal–Wallis analysis of variance to the whole PM_{10} dataset for the sites in the Po Valley (except for the province of BL). TC, K^+, Cl^-, levoglucosan, Σ_8PAHs and SIA were significantly higher ($p < 0.05$) on January 6th than on the other days. Despite the apparent increase in all BB tracers during the episode, the relative percentages of the major PM components did not differ markedly during the study period, however, as it emerged from the analyses of the average chemical compositions of both PM_{10} and $PM_{2.5}$ (Fig. 4 and SI Fig. 13, respectively). The unaccounted masses were obtained as the difference in concentration between the experimentally measured PM_x and the sum of the chemical component analyzed. Other TC components were then computed as the difference between the concentrations of TC and the sum of levoglucosan and Σ_8PAHs. Other ions include F^-, Cl^-, PO_4^{3-}, Na^+, Mg^{2+} and Ca^{2+}.

TC was generally the main component of $PM_{2.5}$ during the study period in all the provinces (SI Fig. 13), with percentages ranging from 27% to 53% (average 37%), followed by nitrate (6%–26%, average 15%), ammonium (2%–9%, average 5%) and sulfate (2%–5%, average 3%); SIA thus accounted for 10%–39%, average 24%. These values appear in line with those reported elsewhere for the Po Valley, e.g., Lombardy (Lonati et al., 2007; Perrone et al., 2012), Piedmont (Piazzalunga et al., 2013) and Veneto (Squizzato et al., 2012). From a spatial point of view, TC generally accounted for the highest proportion of $PM_{2.5}$ in the province of BL (47%), followed by VE (40%), TV (37%), PD and RO (34%) and VI (33%). SIA compounds followed the order: VI (30%) > RO (29%) > VE (26%) > PD (25%) > TV (17%) > BL (15%). Results clearly indicate that the TC content in $PM_{2.5}$ decreases slightly from the mountain valleys to the Po Valley floor and from the coastal to the continental environments.

As for the chemical composition of PM_{10}, results were similar to those of $PM_{2.5}$ (Fig. 4). TC was generally the main PM_{10} constituent in the study period in all the provinces, with percentages ranging from 24% to 47% (average 35%), followed by SIA (11%–37%, average 21%), with the following components: NO_3^- (7%–25%, average 14%); NH_4^+ (2%–8%, average 4%); SO_4^{2-} (2%–5%, average 3%). Results seem similar

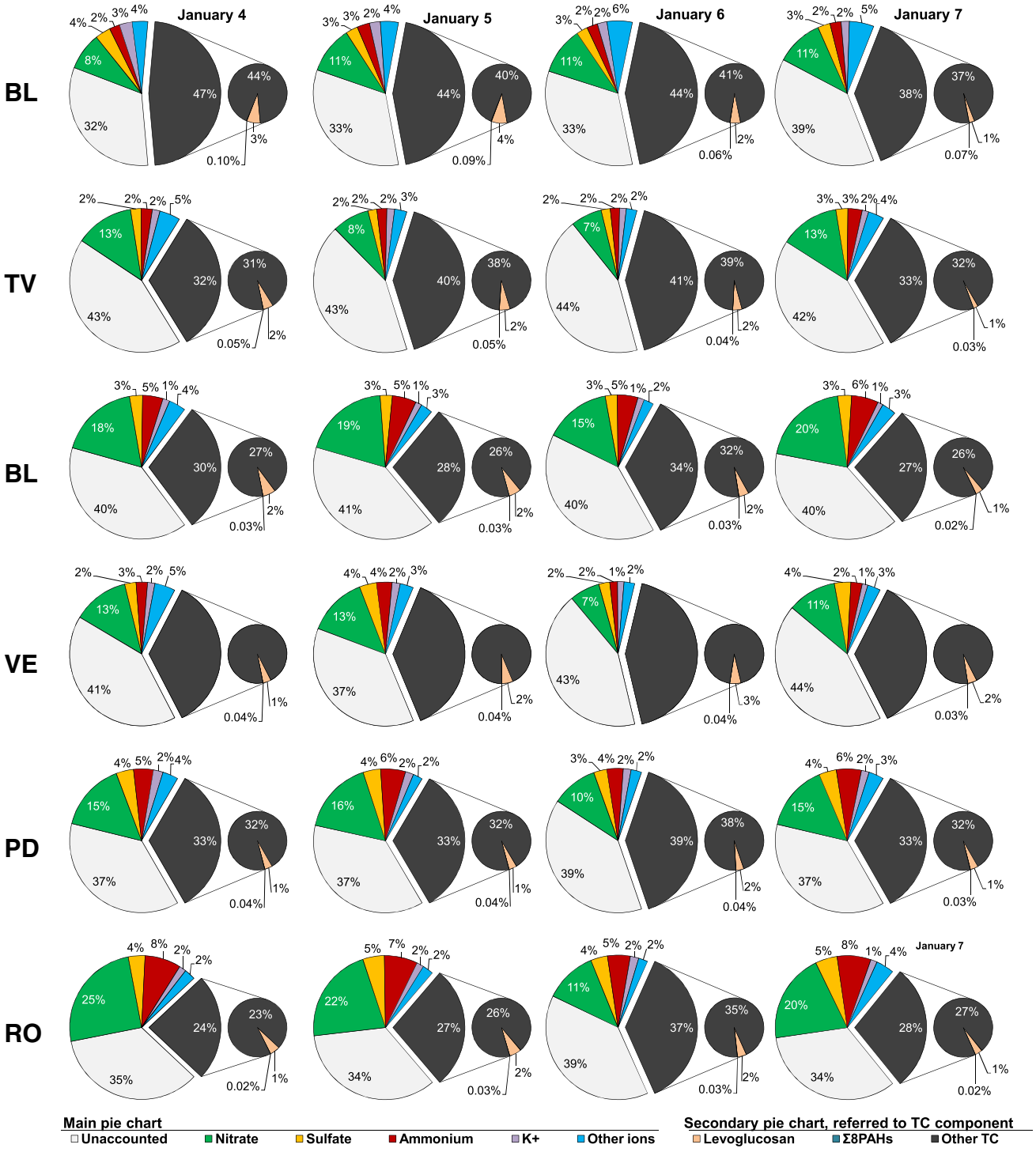

Fig. 4. Average chemical compositions of $PM_{2.5}$ in Veneto. Main pie charts refer to the $PM_{2.5}$ bulk composition and include: total carbon (black); nitrate (green); sulfate (yellow); ammonium (red); K^+ (violet); others ions, i.e. F^-, Cl^-, PO_4^{3-}, Na^+, Mg^{2+} and Ca^{2+}. Secondary pie charts refer to the total carbon component and include: levoglucosan (pink); Σ_8PAHs (dark blue) and other TC components computed as the difference between TC and the sum of levoglucosan and Σ8PAHs concentrations. Note that no data are available for January 6 in the province of VE.

to $PM_{2.5}$ in terms of spatial distribution, with TC generally accounting for the most PM_{10} in the province of BL (43%), followed by VE and TV (37%), PD (35%), RO and VI (29%). SIA followed the order: RO (31%) > VI (26%) > PD (23%) > VE (17%) > TV and BL (15%).

In fact, the SIA components increased unexpectedly during the study period, as no concurrent rises in the levels of the precursor gases (NO, NO_2, NO_x and SO_2) were detected during the event, even though these are reportedly often emitted during open and domestic BB (Akagi et al., 2011). A possible explanation should be sought in the SIA nucleation mechanisms. Kleeman et al. (1999) reported that the particle mass distributions from various wood smoke sources have a single mode that peaks at approximately 100–200 nm and these primary particles are expected to increase their hygroscopic properties with aging (Martin et al., 2013). Soot emitted from the fires, as well as other

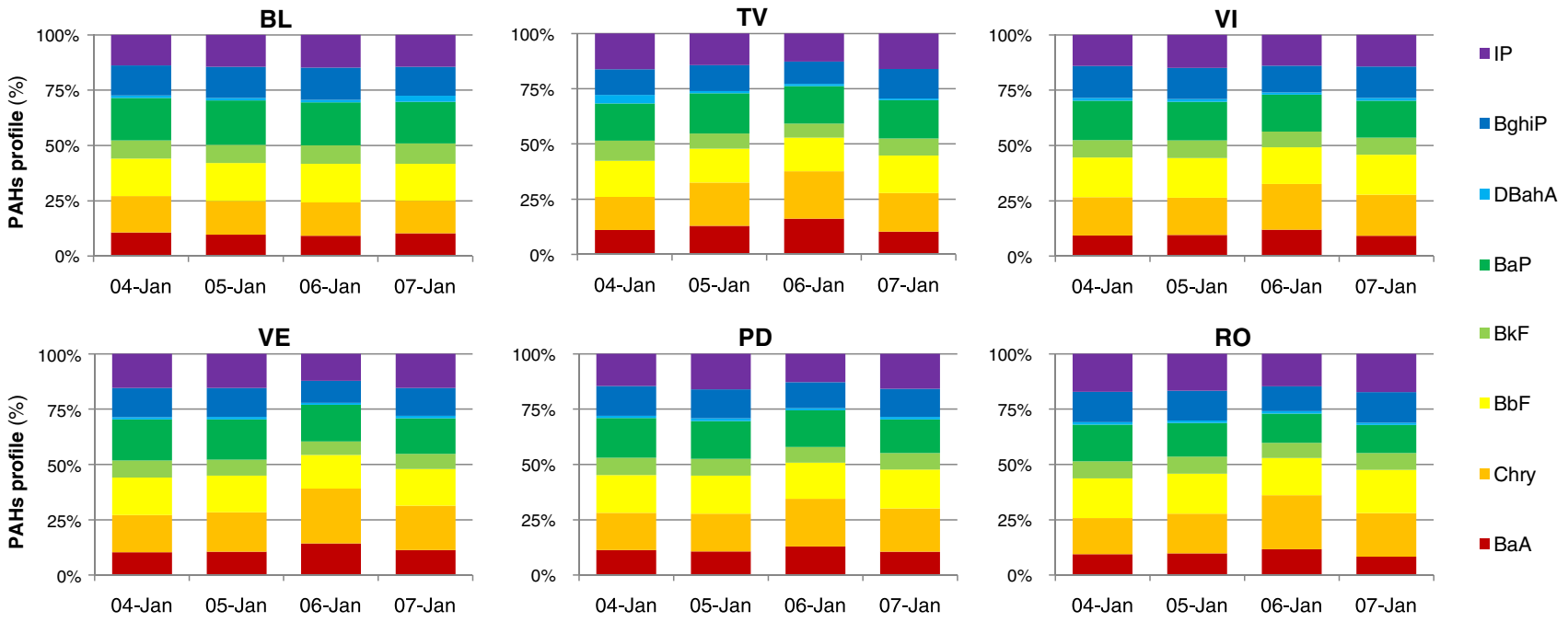

Fig. 5. Average PAH profiles (percent contribution of each analyzed congener to Σ_8PAHs). Data refer to both $PM_{2.5}$ and PM_{10} samples and are grouped by provinces and days.

combustion by-products, could act as condensation nuclei resulting in particles coated with sulfate and nitrate secondary aerosols. This assumption is further supported by the subsequent source apportionment analysis.

4.5. PAHs

PAHs are mainly produced by incomplete combustion and pyrolysis of organic material and are human carcinogens graded as *known* (BaP), *probable* (DBahA) or *possible* (BaA, Chry, BbF, BkF, IP) (IARC, 2010). They reached worrying levels during the event: on January 6th BaP reached the highest concentration of 23.3 and 21.1 ng m^{-3} in the provinces of VE and TV, while the Σ_8PAHs levels were 143 and 129 ng m^{-3}. Fig. 5 shows the PAH profiles (percent contribution of each congener analyzed to Σ_8PAHs). The profiles generally show very similar percentages of congeners between the provinces, as recently reported in other studies on the Veneto (Masiol et al., 2013). The most abundant congener on a regional scale was chrysene (18%), followed by BaP, BbBF (17%), IP (15%), BghiP (13%), BaA (11%) and DBahA (1%). In the province of BL, which was not affected by the event, the profiles maintained constant proportions during the study period. In contrast, significant increases in the percentages of the two lighter congeners (BaA and Chry) were recorded in all the other provinces, with increases of up to 8% for chrysene and up to 5% for BaA from January 4th to January 6th. These results seem to confirm previous findings in Veneto identifying the lighter PM-bound congeners as being emitted by domestic heating, including wood combustion (Masiol et al., 2012).

4.6. PM_x source apportionment

To detect the main PM_x sources on a regional level, the $PM_{2.5}$ and PM_{10} datasets were used as input for two Varimax rotated factor analyses. The datasets include 8 variables (the main compounds analyzed) and 38 and 84 cases, respectively, (samples collected at all sites and on all days). Since levoglucosan and PAHs form part of the TC, they have a non-linearly independent relationship, so a new TC variable was computed for use in the factor analysis by subtracting the masses of these organic species. The results were very similar and are shown in Table 3. Two factors with eigenvalues >1 were extracted for both $PM_{2.5}$ and PM_{10} explaining 90% and 92% of the total variance, respectively. The first factor (49% and 55% of the total variance, respectively) mainly links (loadings >0.6) Cl^-, K^+, TC, levoglucosan and Σ_8PAHs and secondarily (loadings 0.4–0.6) SO_4^{2-}: It clearly reflects the typical BB fingerprint. Since nitrates, sulfates and ammonium are also emitted as primary species from wood combustion (e.g., McDonald et al., 2000), their moderate positive loadings in this factor are not surprising. However, it was reported that those ions are not the major compounds in wood smoke and their importance as primary species from wood combustion is limited compared to the carbon species (Schmidl et al., 2008). Moreover, as hygroscopic properties of wood burning emissions increase with aging (e.g., Heringa et al., 2011; Martin et al., 2013), there may be an uptake of inorganic salts on pre-existing soot particles when particles become more oxidized. This was particularly evident for sulfates and sulfuric acid, which commonly coated the soot particles (e.g., Adachi and Buseck, 2008; Adachi et al., 2010). The second factor (41% and 37%, respectively) is composed mainly of SIA components (NO_3^-, SO_4^{2-}, NH_4^+) and associated with the formation of ammonium sulfate and ammonium nitrate starting from well known precursor gases, i.e. NH_3, SO_2 and NO_x. The presence of significant loadings of potassium in this factor can be accounted for by the formation of mixed salts through heterogeneous reactions: this is particularly evident during brown-haze events, where K-rich particles are recognized as one of the most abundant inorganic aerosol constituents (Li et al., 2010) and are regarded as tracers of biomass burning emissions (Reid et al., 2005; Adachi and Buseck, 2008). The moderate positive loadings of TC and Σ_8PAHs in this factor may be due to the secondary organic aerosol condensation on salt particles (e.g., Hallquist et al., 2009) and the subsequent uptake of semi-volatile organic compounds, such as PAHs, driven by the dilution effect (Lipsky and Robinson, 2006; Donahue et al., 2006). Then the source contributions to the PM_{10} mass was quantified by applying a MLRA, using PM_{10} as the dependent variable and the absolute factor scores as independent variables. This source apportionment method is described elsewhere (Thurston and Spengler, 1985). A very high coefficient of adjusted multiple determination ($R^2_{adj} = 0.97$) was obtained between the measured and modeled PM_{10} data, demonstrating the applicability of the analysis. Results arranged by province and day are shown in Fig. 6. Results for BL confirm that no differences in PM_{10} composition were detectable during the pollution event. The direct effects of BB emissions were mainly evident for VE and TV: the daily increases in BB mass in VE were +27 μg m^{-3} and +118 μg m^{-3} for January 5th and 6th, respectively, while in TV they were +84 and +37 μg m^{-3}. Increases in BB for VI, PD and RO were only seen on January 6th (+35, +85 and +74 μg m^{-3}, respectively). The other source was dominant in RO and VI throughout the study period and moderate to large increases in its mass on January 6th were observed in all the provinces, except for VE. Results confirm that direct BB emissions were the main sources responsible for much of the particulate mass in TV and VE, where more fires were burned, whereas secondary components accounted for most of PM masses in the other provinces.

Table 3
Results of the Varimax rotated factor analyses on $PM_{2.5}$ (left) and PM_{10} (right) datasets. Most significant factor loading (>0.6) are in bold, loadings ranging from 0.4 to 0.6 are in italic.

$PM_{2.5}$	Factor 1	Factor 2	PM_{10}	Factor 1	Factor 2
Cl^-	**0.75**	*0.54*	Cl^-	**0.77**	*0.45*
NO_3^-	0.22	**0.94**	NO_3^-	0.27	**0.93**
SO_4^{2-}	*0.38*	**0.82**	SO_4^{2-}	*0.58*	**0.75**
NH_4^+	0.25	**0.95**	NH_4^+	0.20	**0.97**
K^+	**0.81**	*0.55*	K^+	**0.85**	*0.45*
TC	**0.87**	*0.41*	TC	**0.92**	0.35
Levoglucosan	**0.89**	0.12	Levoglucosan	**0.91**	0.20
Σ_8PAHs	**0.94**	0.23	Σ_8PAHs	**0.96**	0.16
Total var. (%)	49	41	Total var. (%)	55	37
Cum. var. (%)	49	90	Cum. var. (%)	55	92

4.7. Relationships linking the chemical species

Although factor analyses clearly show a component linked to the BB emissions, the relationships between their tracers were investigated in more detail: the scatterplots in Fig. 7 show pairs of relationships between the main components of factor 1 and factor 2 in both $PM_{2.5}$ and PM_{10} samples. The coefficients of determination (R sq) describing how well the regression lines or curves fit the set of data are also provided in Fig. 7 and demonstrate the goodness of the fits. All the BB tracers showed strong linear or exponential relationships with one another and with the PM masses.

Although the highest values of all the chemical species in factor 1 (left) were recorded on January 5th and 6th (triangles and dots, respectively), it is noteworthy that their ratios remained almost constant throughout the study period. This result was already apparent from the chemical speciation (Fig. 4 and SI Fig. 13) and confirms that the average relative chemical composition of the PM was not modified by the emissions from the fires. Another intriguing finding is that no significant changes in the relationship between the chemical species were seen in the whole region during the pollution episode, showing that the average composition of PMx in the Veneto is almost constant and uniform both on the days affected by the pollution event and on the previous ones.

The ratios between the SIA components (upper right) are also shown in Fig. 7 and highlight the significant relationship between ammonium and the sulfate + nitrate equivalents (R sq = 0.93). Since

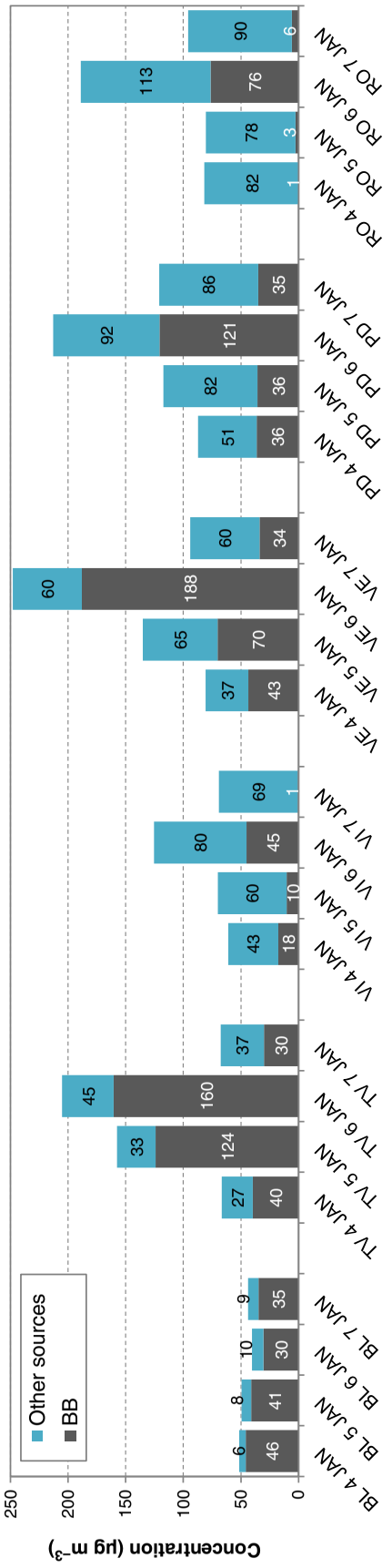

Fig. 6. Results of the source apportionment for PM_{10}. Gray bars indicate BB (factor 1), blue SIA (factor 2). Numbers within bars refer to the apportioned masses ($\mu g\ m^{-3}$).

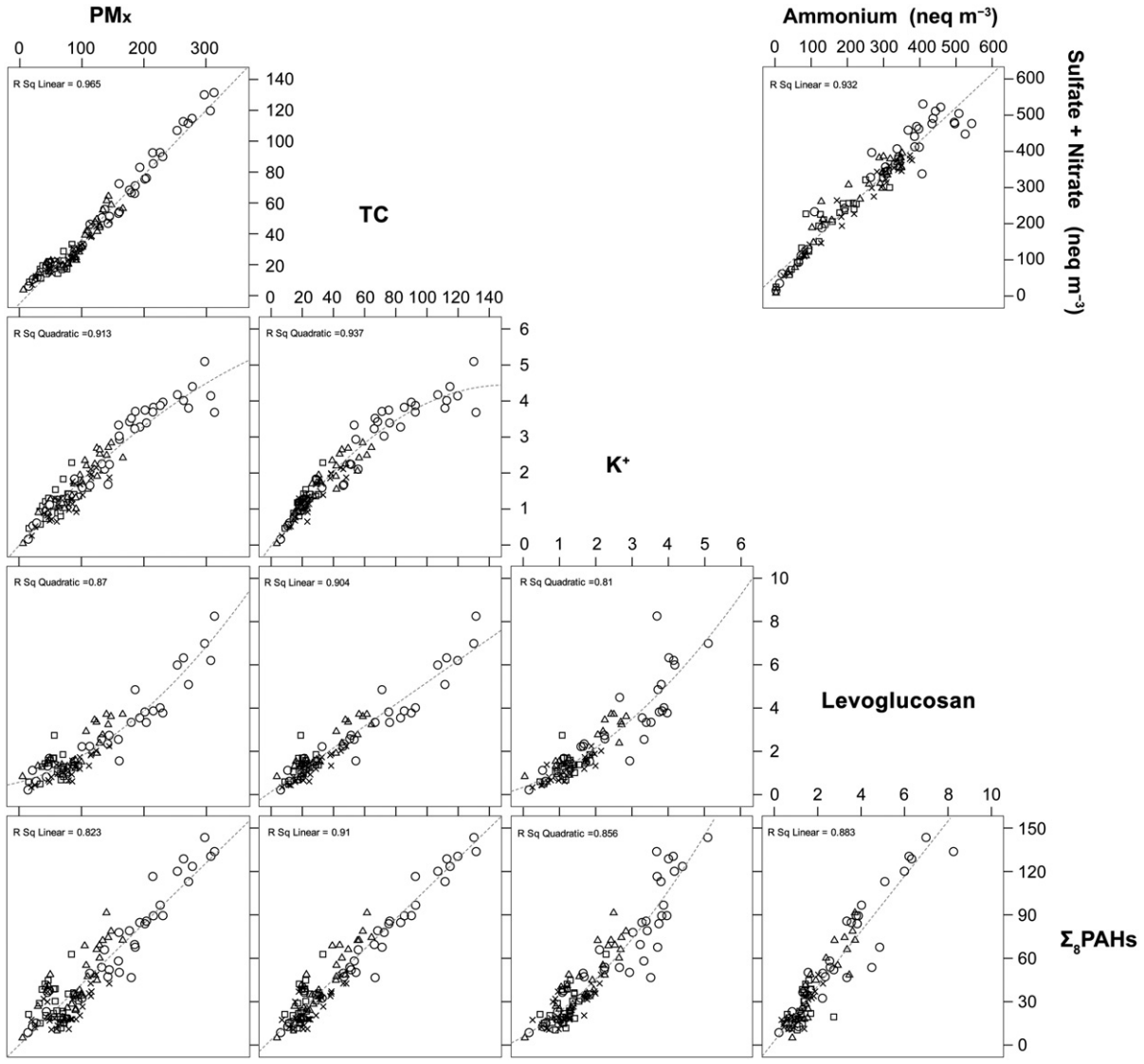

Fig. 7. Pairs of scatter plots between PMx, TC and biomass burning tracers. Data of PM_x, TC, K^+ and levoglucosan are in μg m^{-3}, Σ_8PAHs in ng m^{-3}, ammonium and sulfate + nitrate in neq m^{-3}. Squares refer to samples collected on January 4th, triangles on January 5th, dots on January 6th and crosses on January 7th. R sq is the squared coefficient of determination obtained for the fitted curves.

ammonium is recognized as the main limiting ion for SIA generation (Erisman and Schaap, 2004) and the regression slope was ~1, these results indicate that NH_4^+ almost completely neutralizes SO_4^{2-} and NO_3^- throughout the region.

4.8. Pollutant dispersion and its effects in the Po Valley

Due to the weather conditions during the event, i.e. the no rainfall, slow winds and low mixing heights, the effect of the fires could be expected to be recorded in the neighboring regions too. The levels of $PM_{2.5}$ and PM_{10} measured at 51 and 133 sites, respectively in the Veneto (16 and 41 sites, respectively), Lombardy (13 and 35), Emilia Romagna (22 and 42) and Friuli Venezia Giulia (none and 15) were used to ascertain the pollutant dispersion and its effects in the Po Valley. Data were provided by the local environmental agencies, obtained from both automatic and manual sampling stations. Since the sole purpose of this data processing was to describe the extent of the pollution episode's effects on air quality over a very wide area, no distinction was drawn for the site categories. An exhaustive list of the sampling stations used is given in SI Tables 2 and 3. Data were then spatially interpolated using the inverse distance weighting method (IDW, power: 2, n. of points: 5) method and the results are shown in Fig. 8 (PM_{10}) and SI Fig. 14 ($PM_{2.5}$).

Maps for January 4th show relatively uniform concentrations of both $PM_{2.5}$ and PM_{10} throughout the Po Valley, with slightly higher values measured over the Milan metropolitan area and some provinces of Veneto (TV, VE, PD, VR): $PM_{2.5}$ concentrations ranged between 60 and 80 μg m^{-3} and PM_{10} between 80 and 100 μg m^{-3}. The effect of the fires was clearly apparent on January 5th, when evident increases in PM_x levels were recorded over the TV and VE provinces ($PM_{2.5}$ and PM_{10} levels > 100 μg m^{-3}). In the other areas of the Po Valley, PM_x concentrations remained similar to the previous day. On January 6th the pollution event reached the highest levels, in boththe extent and concentrations: $PM_{2.5}$ reached 263 μg m^{-3} in the TV province and levels above 100 μg m^{-3} in large part of the Veneto and in the northern areas of Emilia-Romagna. Similarly, PM_{10} reached the highest concentrations in Marcon, a village between the VE and TV provinces (316 μg m^{-3}), Venice-Mestre (313 μg m^{-3}) and Treviso (273 μg m^{-3}). PM_{10} data are also available for the Friuli Venezia Giulia region, where very high values were measured at the stations closer to the Veneto, e.g. Brugnera (264 μg m^{-3}). PM_{10} concentrations above 100 μg m^{-3} were also measured in Lombardy. On January 7th, a general marked

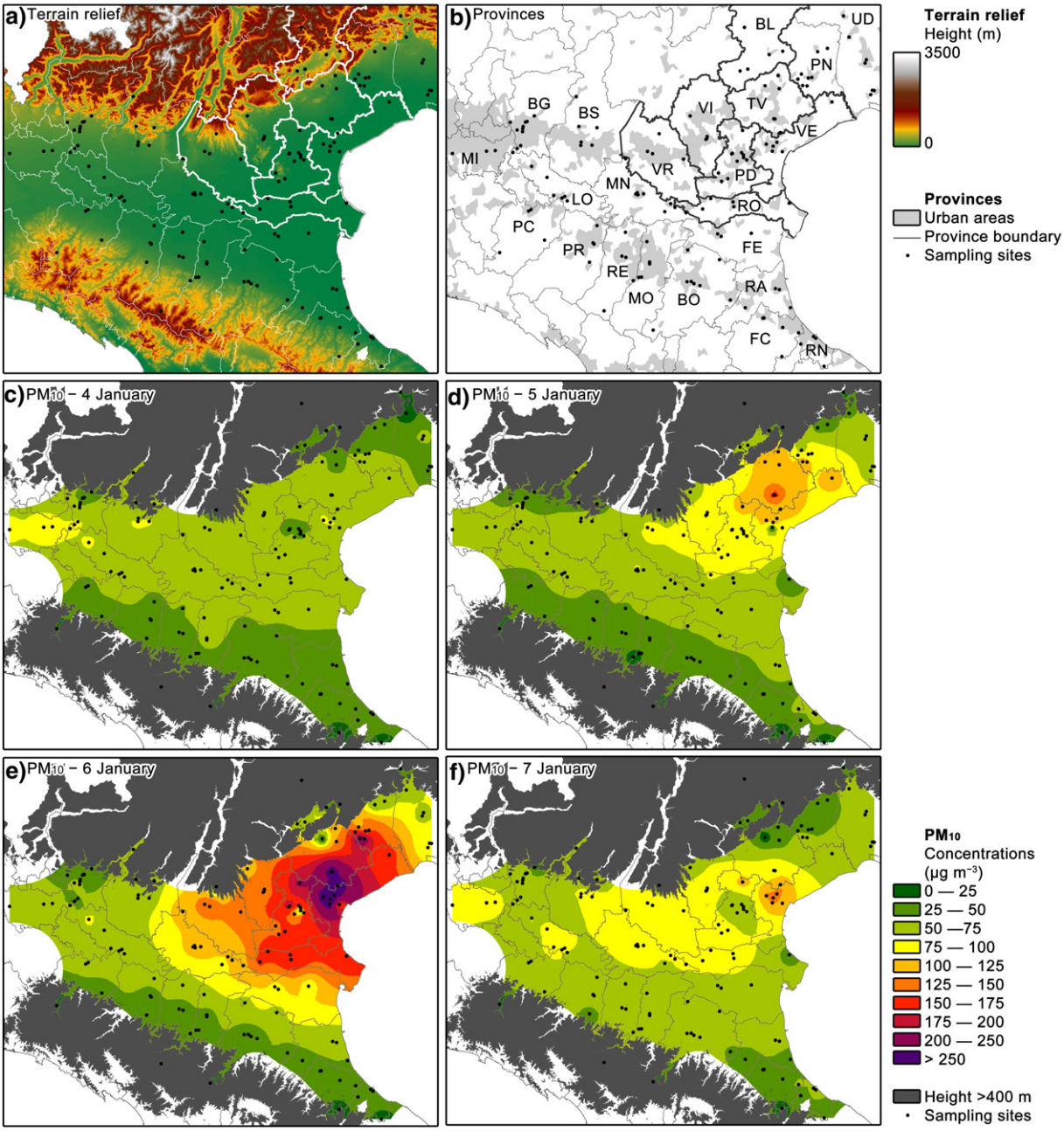

Fig. 8. Results of the spatial interpolation for PM_{10}.

decrease in the concentrations was observed, although $PM_{2.5}$ levels above 100 μg m^{-3} were recorded in the province of VR and PM_{10} levels between 100 and 200 μg m^{-3} in the provinces of VE, PD and TV and on the border between Veneto and Lombardy.

Finally, the HYSPLIT model was used to simulate the potential transport pathway of the pollution event. The 48 h forward simulations were computed every 2 h from January 5th at 18:00 UTC to January 6th at 15:00 UTC, i.e. the period with the highest hourly PM_{10} levels. Results are given in SI Fig. 15 as a frequency plot and show that the most frequent trajectories moved to the south-east. This shows that the decrease in the levels of particulate air pollution after the episode could be due to the advection of the polluted air masses towards the Adriatic Sea: on January 7th, the $PM_{2.5}$ and PM_{10} returned to low levels in most of the Veneto Region.

5. Conclusions

A widespread and intense air pollution event in the eastern Po Valley was monitored and the main results can be summarized as follows:

- The effects of folk fires were recorded shortly after the piles were lit and caused a very sharp increase in PM_{10} concentrations for a ~20 h period, then concentrations fell to the levels recorded before the fires were lit;
- The pollution event was only detected in the lowlands, while the lighting of fires did not generate abnormal concentrations in the alpine valleys;
- The increased levels of $PM_{2.5}$ and PM_{10} pollution due to the fires were estimated in major cities using a multiple linear regression analysis.

Results show increases of daily particulate matter ranging from 90 to 235 μg m^{-3} of $PM_{2.5}$ and from 65 to 200 μg m^{-3} of PM_{10} in the lowland territories on January 6th;
- Multivariate source apportionment revealed that biomass burning was a dominant PM source over all the region, mainly in VE and TV provinces;
- PM, total carbon, PAHs and the biomass burning tracers correlated very well throughout the territory and most of the sampling stations showed very similar ratios even they were located in environments of different category. It can be concluded that the biomass burning pollution affected similarly all the lowland parts of the region;
- As expected, the concentrations of typical biomass burning tracers significantly increased at all sites of the Po Valley on January 6th, but a significant simultaneous increase in secondary inorganic components has been detected. Emissions of primary soot particles and byproducts of wood combustion during the event probably acted as condensation nuclei for secondary processes. That is why the episode contributed to raising of PM_x levels both directly and indirectly, by providing condensation nuclei for the formation of ammonium nitrate and ammonium sulfate aerosols.
- Pollutant dispersion during the study period was assessed by analyzing the $PM_{2.5}$ and PM_{10} concentrations at various sites in the Po Valley. Results show that the effects of the episode were recorded in most of northern Italy and forward trajectory analysis also showed that the pollution plume moved towards the Adriatic Sea.

Disclaimer

The views expressed in this study are exclusively of the authors and may not reflect those of ARPAV.

Acknowledgments

This study is the result of a cooperation between the Ca' Foscari University of Venice and ARPAV. The authors are grateful to ARPA Emilia-Romagna (http://www.arpa.emr.it/) and ARPA Friuli Venezia Giulia (http://www.arpa.fvg.it/) for providing PM data of their monitoring stations via websites, and Dr. Vorne Giannelle and Dr. Cristina Colombi (ARPA Lombardia) for providing data of Lombardy. ARPAV-Centro Meteorologico di Teolo provided some weather data. The authors also gratefully acknowledge the NOAA Air Resources Laboratory (ARL) for the provision of the HYSPLIT transport and dispersion model used in this publication.

Appendix A. Supplementary data

Supplementary data to this article can be found online at http://dx.doi.org/10.1016/j.scitotenv.2013.12.077.

References

Adachi K, Buseck PR. Internally mixed soot, sulfates, and organic matter in aerosol particles from Mexico City. Atmos Chem Phys 2008;8(21):6469–81.
Adachi K, Chung SH, Buseck PR. Shapes of soot aerosol particles and implications for their effects on climate. J Geophys Res 2010;115(D15). http://dx.doi.org/10.1029/2009JD012868.
Akagi SK, Yokelson RJ, Wiedinmyer C, Alvarado MJ, Reid JS, Karl T, et al. Emission factors for open and domestic biomass burning for use in atmospheric models. Atmos Chem Phys 2011;11:4039–72.
Alves CA, Gonçalves C, Pio CA, Mirante F, Caseiro A, Tarelho L, et al. Smoke emissions from biomass burning in a Mediterranean shrubland. Atmos Environ 2010;44(25):3024–33.
Andreae MO, Merlet P. Emission of trace gases and aerosols from biomass burning. Global Biogeochem Cycles 2001;15(4):955–66.
Arey J, Atkinson R. Photochemical reactions of PAHs in the atmosphere. In: Douben PET, editor. PAHs: an ecotoxicological perspective. Chichester: Wiley; 2003. p. 47–63.
ARPAV (Environmental Protection Agency of Veneto Region). Regional report of air quality—year 2011; 2012 [in Italian].
Belis CA, Cancelinha J, Duane M, Forcina V, Pedroni V, Passarella R, et al. Sources for PM air pollution in the Po Plain, Italy: I. Critical comparison of methods for estimating biomass burning contributions to benzo(a)pyrene. Atmos Environ 2011;45(39):7266–75.
Caseiro A, Bauer H, Schmidl C, Pio AC, Puxbaum H. Wood burning impact on PM10 in three Austrian regions. Atmos Environ 2009;43:2186–95.
CEN (Comité Européen de Normalisation). Air quality — determination of suspended particulate matter-reference method and field test procedure to demonstrate reference equivalence of measurements methods. EN 12341:1998. CEN; 1998.
CEN (Comité Européen de Normalisation). Ambient air quality — standard gravimetric measurements for the determination of the PM2.5 mass fraction of suspended particulate matter. EN 14907:2005. CEN; 2005a.
CEN (Comité Européen de Normalisation). Ambient air quality — standard method for measurement of benzene concentrations. Automated pumped sampling with in situ gas chromatography. EN 14662-3: 2005. CEN; 2005b.
CEN (Comité Européen de Normalisation). Air quality — standard method for the measurement of the concentration of benzo[a]pyrene in ambient air. EN 15549:2008. CEN; 2008.
CEN (Comité Européen de Normalisation). Ambient air — standard method for the measurement of the concentration of carbon monoxide by non-dispersive infrared spectroscopy. EN 14626:2012. CEN; 2012a.
CEN (Comité Européen de Normalisation). Ambient air — standard method for the measurement of the concentration of nitrogen dioxide and nitrogen monoxide by chemiluminescence. EN 14211:2012. CEN; 2012b.
CEN (Comité Européen de Normalisation). Ambient air — standard method for the measurement of the concentration of sulphur dioxide by ultraviolet fluorescence. EN 14212:2012. CEN; 2012c.
CEN (Comité Européen de Normalisation). Ambient air — standard method for the measurement of the concentration of ozone by ultraviolet photometry. EN 14625:2012. CEN; 2012d.
Crutzen PJ, Andreae MO. Biomass burning in the tropics: Impact on atmospheric chemistry and biogeochemical cycles. Science 1990;250:1669–78.
de Leeuw F, Horálek J. Assessment of the health impacts of exposure to PM2.5 at a European level. Bilthoven, NL: ETC./ACC Technical Paper 2009/1; 2009 [Available at: http://acm.eionet.europa.eu/reports/ETCACC_TP_2009_1_European_PM2.5_HIA].
Donahue NM, Robinson AL, Stanier CO, Pandis SN. Coupled partitioning, dilution, and chemical aging of semivolatile organics. Environ Sci Technol 2006;40(8):2635–43.
Draxler RR, Rolph GD. HYSPLIT (HYbrid Single-Particle Lagrangian Integrated Trajectory) Model access via NOAA ARL READY Website (http://ready.arl.noaa.gov/HYSPLIT.php). Silver Spring, MD: NOAA Air Resources Laboratory; 2013.
EEA, European Environment Agency. AirBasedThe European Air Quality Database. Available from: http://www.eea.europa.eu/themes/air/airbase. [last accessed January, 2013].
Erisman JW, Schaap M. The need for ammonia abatement with respect to secondary PM reductions in Europe. Environ Pollut 2004;129:159–63.
European Pellet Council. Statistical Report; 2011. Available from: http://www.pelletcouncil.eu/en/statistics/.
Fine PM, Cass GR, Simoneit BRT. Chemical characterization of fine particle emissions from fireplace combustion of woods grown in the northeastern United States. Environ Sci Technol 2001;35:2665–75.
Gelencsér A, May B, Simpson D, Sánchez-Ochoa A, Kasper-Giebl A, Puxbaum H, et al. Source apportionment of PM2.5 organic aerosol over Europe: primary/secondary, natural/anthropogenic, fossil/biogenic origin. J Geophys Res 2007;112:D23S04. http://dx.doi.org/10.1029/2006JD008094.
Gustafsson O, Krusa M, Zencak Z, Sheesley RJ, Granat L, Engstrom E, et al. Brown clouds over South Asia: Biomass or fossil fuel combustion? Science 2009;323:495–8.
Hallquist M, Wenger JC, Baltensperger U, Rudich Y, Simpson D, Claeys M, et al. The formation, properties and impact of secondary organic aerosol: current and emerging issues. Atmos Chem Phys 2009;9:5155–236.
Hennigan CJ, Sullivan AP, Collett Jr JL, Robinson AL. Levoglucosan stability in biomass burning particles exposed to hydroxyl radicals. Geophys Res Lett 2010;37(L09806):4.
Heringa MF, DeCarlo PF, Chirico R, Tritscher T, Dommen J, Weingartner E, et al. Investigations of primary and secondary particulate matter of different wood combustion appliances with a high-resolution time-of-flight aerosol mass spectrometer. Atmos Chem Phys 2011;11:5945–57.
IARC (International Agency for Research on Cancer). Some non-heterocyclic polycyclic aromatic hydrocarbons and some related exposures. IARC Monogr Eval Carcinog Risks Hum 2010;92. [Lyon: IARC].
ISO (International Organization for Standardization). Ambient air — determination of particle-phase polycyclic aromatic hydrocarbons by high performance liquid chromatography. ISO 16362: 2005. ISO; 2005.
Keywood M, Kanakidou M, Stohl A, Dentener F, Grassi G, Meyer CP, et al. Fire in the air — biomass burning impacts in a changing climate. Crit Rev Environ Sci Technol 2011;43:40–83.
Kleeman MJ, Schauer JJ, Cass GR. Size and composition distribution of fine particulate matter emitted from wood burning, meat charbroiling, and cigarettes. Environ Sci Technol 1999;33(20):3516–23.
Koppmann R, von Czapiewski K, Reid JS. A review of biomass burning emissions, part I: gaseous emissions of carbon monoxide, methane, volatile organic compounds, and nitrogen containing compounds. Atmos Chem Phys Discuss 2005;5:10455–516.
Laumbach RJ, Kipen HM. Respiratory health effects of air pollution: update on biomass smoke and traffic pollution. J Allergy Clin Immunol 2012;129(1):3–11.
Lewis AC, Evans MJ, Hopkins JR, Punjabi S, Read KA, Purvis RM, et al. The influence of biomass burning on the global distribution of selected non-methane organic compounds. Atmos Chem Phys 2013;13:851–67.
Li WJ, Shao LY, Buseck PR. Haze types in Beijing and the influence of agricultural biomass burning. Atmos Chem Phys 2010;10(17):8119–30.

Lipsky EM, Robinson AL. Effects of dilution on fine particle mass and partitioning of semivolatile organics in diesel exhaust and wood smoke. Environ Sci Technol 2006;40(1):155–62.
Lonati G, Ozgen S, Giugliano M. Primary and secondary carbonaceous species in PM2.5 samples in Milan (Italy). Atmos Environ 2007;41(22):4599–610.
Martin M, Tritscher T, Jurányi Z, Heringa MF, Sierau B, Weingartner E, et al. Hygroscopic properties of fresh and aged wood burning particles. J Aerosol Sci 2013;56:15–29.
Masiol M, Hofer A, Squizzato S, Piazza R, Rampazzo G, Pavoni B. Carcinogenic and mutagenic risk associated to airborne particle-phase polycyclic aromatic hydrocarbons: a source apportionment. Atmos Environ 2012;60:375–82.
Masiol M, Formenton G, Pasqualetto A, Pavoni B. Seasonal trends and spatial variations of PM10-bounded polycyclic aromatic hydrocarbons in Veneto Region, Northeast Italy. Atmos Environ 2013;79:811–21.
Mayol-Bracero OL, Guyon P, Graham B, Roberts G, Andreae MO, Decesari S, et al. Water-soluble organic compounds in biomass burning aerosols over Amazonia, 2, apportionment of the chemical composition and importance of the polyacidic fraction. J Geophys Res 2001;107(D20):8091. http://dx.doi.org/10.1029/2001JD000522.
Mazzoleni LR, Zielinska B, Moosmuller H. Emissions of levoglucosan, methoxy phenols, and organic acids from prescribed burns, laboratory combustion of wildland fuels, and residential wood combustion. Environ Sci Technol 2007;41:2115–22.
McDonald JD, Zielinska B, Fujita EM, Sagebiel JC, Chow JC, Watson JG. Fine particle and gaseous emission rates from residential wood combustion. Environ Sci Technol 2000;34(11):2080–91.
Muhle J, Lueker J, Su Y, Miller BR, Prather KA, Weiss RF. Trace gas and particulate emissions from the 2003 southern California wildfires. J Geophys Res Atmos 2007;112:D03307. http://dx.doi.org/10.1029/2006JD007350.
NCEP (National Centers for Environmental Prediction). EMC Model Documentation. Available from: http://www.emc.ncep.noaa.gov/modelinfo/index.html. [last accessed August, 2013].
Pastorello C, Caserini S, Galante S, Dilara P, Galletti F. Importance of activity data for improving the residential wood combustion emission inventory at regional level. Atmos Environ 2011;45(17):2869–76.
Pecorari E, Squizzato S, Masiol M, Radice P, Pavoni B, Rampazzo G. Using a photochemical model to assess the horizontal, vertical and time distribution of PM2.5 in a complex area: relationships between the regional and local sources and the meteorological conditions. Sci Total Environ 2013;443:681–91.
Perrone MG, Larsen BR, Ferrero L, Sangiorgi G, De Gennaro G, Udisti R, et al. Sources of high PM2.5 concentrations in Milan, Northern Italy: molecular marker data and CMB modeling. Sci Total Environ 2012;414:343–55.
Piazzalunga A, Fermo P, Bernardoni V, Vecchi R, Valli G, De Gregorio MA. A simplified method for levoglucosan quantification in wintertime atmospheric particulate matter by high performance anion-exchange chromatography coupled with pulsed amperometric detection. Int J Environ Anal Chem 2010;90:934–47.
Piazzalunga A, Belis C, Bernardoni V, Cazzuli O, Fermo P, Valli G, et al. Estimates of wood burning contribution to PM10 in Lombardy (Po Valley, Italy) using different approaches. Atmos Environ 2011;45:6642–9.
Piazzalunga A, Anzano M, Collina E, Lasagni M, Lollobrigida F, Pannocchia A, et al. Contribution of wood combustion to PAH and PCDD/F concentrations in two urban sites in Northern Italy. J Aerosol Sci 2013;56:30–40.
Pignatelli T, D'Elia I, Vialetto G, Bencardino M, Contaldi M. The use of biomass: synergies and trade-offs between Climate Change and Air Pollution, Italy. 17th Annual International Emission Inventory Conference. Portland, OR: US Environmental Protection Agency; 2008.
Pio CA, Legrand M, Alves CA, Oliveira T, Afonso J, Caseiro A, et al. Chemical composition of atmospheric aerosols during the 2003 summer intense forest fire period. Atmos Environ 2008;42(32):7530–43.
Portin H, Mielonen T, Leskinen A, Arola A, Pärjälä E, Romakkaniemi S, et al. Biomass burning aerosols observed in Eastern Finland during the Russian wildfires in summer 2010 — Part 1: in-situ aerosol characterization. Atmos Environ 2012;47:269–78.
Puxbaum H, Caseiro A, Sánchez-Ochoa A, Kasper-Giebl A, Claeys M, Gelencsér A, et al. Levoglucosan levels at background sites in Europe for assessing the impact of biomass combustion on the European aerosol background. J Geophys Res 2007;112:D23S05. http://dx.doi.org/10.1029/2006JD008114.
Radzi AM, Oros DR, Simoneit B. Biomass burning as the main source of organic aerosol particulate matter in Malaysia during haze episodes. Chemosphere 2004;55:1089–95.
Reche C, Viana M, Amato F, Alastuey A, Moreno T, Hillamo R, et al. Biomass burning contributions to urban aerosols in a coastal Mediterranean City. Sci Total Environ 2012;427–428:175–90.
Reid JS, Koppmann R, Eck TF, Eleuterio DP. A review of biomass burning emissions part II: intensive physical properties of biomass burning particles. Atmos Chem Phys 2005;5:799–825.
Rolph GD. Real-time Environmental Applications and Display system (READY) Website (http://ready.arl.noaa.gov). Silver Spring, MD: NOAA Air Resources Laboratory; 2013.
Saarikoski S, Sillanpää M, Sofiev M, Timonen H, Saaenio K, Teinilä K, et al. Chemical composition of aerosols during a major biomass burning episode over northern Europe in spring 2006: experimental and modelling assessments. Atmos Environ 2007;41:3577–89.
Schmidl C, Bauer H, Dattler A, Hitzenberger R, Weissenboeck G, Marr IL, et al. Chemical characterisation of particle emissions from burning leaves. Atmos Environ 2008;42(40):9070–9.
Shafizadeh F. Pyrolysis and combustion of cellulosic materials. Adv Carbohydr Chem 1968;23:419–74.
Simoneit B. Biomass burning—a review of organic tracers for smoke from incomplete combustion. Appl Geochem 2002;17:129–62.
Squizzato S, Masiol M, Innocente E, Pecoarari E, Rampazzo G, Pavoni B. A procedure to assess local and long-range transport contributions to PM2.5 and secondary inorganic aerosol. J Aerosol Sci 2012;46:64–76.
Squizzato S, Masiol M, Brunelli A, Pistollato S, Tarabotti E, Rampazzo G, et al. Factors determining the formation of secondary inorganic aerosol: a case study in the Po Valley (Italy). Atmos Chem Phys 2013;13:1927–39.
Szidat S, Prévôt ASH, Sandradewi J, Alfarra MR, Synal H-A, Wacker L, et al. Dominant impact of residential wood burning on particulate matter in Alpine valleys during winter. Geophys Res Lett 2007;34:L05820. http://dx.doi.org/10.1029/2006GL028325.
Thurston GD, Spengler JD. A quantitative assessment of source contribution to inhalable particulate matter pollution in Metropolitan Boston. Atmos Environ 1985;19:9–25.
Tomasi C. The nocturnal surface inversion height in the Po valley. Atmos Environ 1983;17(6):1123–9.
van Drooge BL, Perez Ballesta P. Seasonal and daily source apportionment of polycyclic aromatic hydrocarbon concentrations in PM10 in a semirural European area. Environ Sci Technol 2009;43:7310–6.
Vecchi R, Marcazzan G, Valli G, Ceriani M, Antoniazzi C. The role of atmospheric dispersion in the seasonal variation of PM1and PM2.5 concentration and composition in the urban area of Milan (Italy). Atmos Environ 2004;38(27):4437–46.
Vecchi R, Marcazzan G, Valli G. A study on nighttime–daytime PM10 concentration and elemental composition in relation to atmospheric dispersion in the urban area of Milan (Italy). Atmos Environ 2007;41(10):2136–44.
Zhang Y, Obrist D, Zielinska B, Gertler A. Particulate emissions from different types of biomass burning. Atmos Environ 2013;72:27–35.